Proc. Natl. Acad. Sci. USA
Vol. 91, pp. 7164–7168, July 1994
Biochemistry

Tyr-129 is important to the peptide ligand affinity and selectivity of human endothelin type A receptor

(G-protein-coupled receptor/binding site/mutagenesis/receptor subtypes)

JONATHAN A. LEE*†, JOHN D. ELLIOTT‡, JOYCE A. SUTIPHONG*, WESTLEY J. FRIESEN*, ELIOT H. OHLSTEIN§, JEFFREY M. STADEL§, JOHN G. GLEASON‡, AND CATHERINE E. PEISHOFF†¶

Departments of *Macromolecular Sciences, ‡Medicinal Chemistry, §Pharmacology, and ¶Physical and Structural Chemistry, SmithKline Beecham Pharmaceuticals, King of Prussia, PA 19406

Communicated by Sidney Udenfriend, March 25, 1994 (received for review February 16, 1994)

ABSTRACT **Molecular modeling and protein engineering techniques have been used to study residues within G-protein-coupled receptors that are potentially important to ligand binding and selectivity. In this study, Tyr-129 located in transmembrane domain 2 of the human endothelin (ET) type A receptor A (hET_A) was targeted on the basis of differences between the hET_A and type B receptor (hET_B) sequences and the position of the residue on ET receptor models built using the coordinates of bacteriorhodopsin. Replacement of Tyr-129 of hET_A by alanine, glutamine, asparagine, histidine, lysine, serine, or phenylalanine results in receptor variants with enhanced ET-3 and sarafotoxin 6C affinities but with unchanged ET-1 and ET-2 affinities. Except for Tyr-129 → Phe hET_A, these hET_A variants have two to three orders of magnitude lower binding affinity for the ET_A-selective antagonist BQ123. Replacement of His-150, the residue in hET_B that is analogous in sequence to Tyr-129 of hET_A, by either tyrosine or alanine does not affect the affinity of peptide ligands. These results indicate that although transmembrane domain 2 is important in ligand selectivity for hET_A, it does not play a significant role in the lack of ligand selectivity shown by hET_B. Chimeric receptors have been constructed that further support these conclusions and indicate that at least two hET_A regions contribute to ligand selectivity. Additionally, the data support an overlap in the binding site in hET_A of agonists ET-3 and sarafotoxin 6C with that of the antagonist BQ123.**

Many pharmacologically important receptors are G-protein coupled and are predicted to have a common secondary structure composed of seven helical transmembrane (TM) domains connected by loops of 15 to >200 residues (1). Determination of the molecular details underlying differences in ligand affinity for this family of receptors is important to understanding the molecular basis of their action and to the design of specific therapeutic agents. Numerous studies have investigated the way in which G-protein-coupled receptors (GPCRs) engage their structurally diverse ligands. For the bioactive amine receptors, the most widely studied class of GPCRs, affinity labeling, site-directed mutagenesis, and fluorescence quenching experiments have implicated the TM receptor domains in ligand binding (for review, see refs. 1–3). More recently, the TM domains of endothelin (ET) (4, 5) and neuromedin B receptors (6) have been demonstrated as important for binding their peptide ligands.

Detailed studies of receptor structure relating to binding and or function for GPCRs are impeded by the lack of high-resolution structural information. Molecular models, however, have been constructed (7–10) using the experimentally determined structure of the TM domains of bacteriorhodopsin (BR) (11), a light-driven proton pump. Although BR does not associate with a heterotrimeric G-protein complex, it is currently the only membrane-bound protein containing seven TM helices for which some structural data are available. The relevance of such models is of concern (12, 13), but comparison of a recent two-dimensional image of rhodopsin (14), a G-protein-coupled photosensor, to BR indicates a highly similar barrel-like disposition of the seven TM helices. GPCR models based on BR are therefore approximate but provide an important starting point in the iterative procedure of model building and structural refinement based on mutagenesis and biochemical data.

The GPCRs that bind the vasoactive isopeptides of ET and sarafotoxin are ideally suited for an investigation of the molecular determinants of ligand binding because large, receptor-subtype-specific differences in binding affinity for the highly homologous ligands are known (15). Currently, two subtypes of ET receptor denoted ET_A and ET_B (59% identity, 78% homology) are recognized (16). The agonist binding profile of ET_A is selective: ET-1 and ET-2 bind with high and similar affinity; ET-3 binds with a 70- to 100-fold lower affinity than ET-1, and sarafotoxin 6C (S6C) binds with >1000-fold lower affinity than ET-1. The ligand-binding profile of ET_B is nonselective: ET-1, ET-2, ET-3, and S6C bind with a high and similar affinity (17). More recently, two ligands that are highly receptor-subtype specific have been described: BQ123, a cyclic peptide antagonist of ET_A; and IRL 1620, a linear agonist peptide of ET_B (18, 19).

In this study, molecular models of human ET_A (hET_A) and human ET_B (hET_B) were used to identify receptor residues that may contribute to either agonist or antagonist affinities and/or selectivities for ET receptors. We found that replacement of Tyr-129 within TM2 of hET_A increases by two orders of magnitude the binding affinity of ET-3 and S6C and decreases by two to three orders of magnitude the binding affinity of BQ123. The ligand selectivity of these hET_A variants resembles that of hET_B. Replacement of the analogous residue in TM2 of hET_B does not affect ligand affinity, indicating a differential role for this region of TM2 in ligand binding to ET receptor subtypes. The affinity changes for hET_A variants indicate that the binding site within TM2 of certain peptide agonists overlaps with that of a peptide antagonist. Additionally, results from ET receptor chimeras suggest that at least two receptor regions contribute to peptide agonist selectivity for hET_A.

MATERIALS AND METHODS

Receptor Modeling. Models for the TM regions of both hET_A and hET_B were built from the BR coordinate set using an

The publication costs of this article were defrayed in part by page charge payment. This article must therefore be hereby marked "*advertisement*" in accordance with 18 U.S.C. §1734 solely to indicate this fact.

Abbreviations: ET, endothelin; ET-*n*, ET-1, 2, or 3; GPCR, G-protein-coupled receptor; hET_A and hET_B, human ET receptor subtype A and B, respectively; S6C, sarafotoxin 6C; TM, transmembrane; BR, bacteriorhodopsin.

†To whom reprint requests should be addressed.

alignment substantially the same as that for bovine ET_A and ET_B previously described (10). The alignment of TM3 was shifted toward the N terminus by one residue to maintain Lys-166(hET_A)/182(hET_B), conserved in both receptor subtypes and implicated in the binding of certain agonist peptides (4, 5), in a cleft accessible to the extracellular surface. The models were generated by residue replacement using the Biopolymers module of the molecular modeling program SYBYL (Version 5.5, Tripos Associates, St. Louis). Obvious side chain steric clashes were removed manually, and TMs 3, 4, and 5 were adjusted slightly for better interhelical interactions. The models were energy minimized using the program AMBER, Version 3.0 (20). Minimization consisted of 1000 steps with a dielectric constant of 80 followed by 1000 steps using a dielectric constant of 10 with a nonbonded cut-off of 10 Å.

Mutagenesis and Receptor Expression. cDNA fragments encoding the open reading frames of hET_A and hET_B (16) were subcloned into vector pRCCMV (Invitrogen) and used for mutagenesis as described by Kunkel *et al.* (21). Mutations were identified by plasmid DNA sequencing using a modified dideoxynucleotide chain-termination method (22) (Sequenase II, United States Biochemical) and confirmed by automated DNA sequencing using an Applied Biosystems model 373 A sequencer. Plasmid DNA was prepared by alkaline lysis and purified by Qiagen (Chatsworth, CA) column chromatography. Human embryonic kidney (HEK) 293 cells (ATCC CRL 1573) were grown in Eagle's minimal medium supplemented with Earle's salts, 10% fetal calf serum, and 1 mM glutamine (EMEM) at 5% CO_2/95% air. Transient transfection of HEK 293 cells was conducted by the calcium phosphate method (23).

Construction of Receptor Chimeras. The cDNA encoding hET_B was altered by site-directed mutagenesis to generate a unique *Hin*cII site that replaced Ile-197 by valine, the corresponding residue in hET_A. The resulting receptor variant, Ile-197 → Val hET_B, has apparent affinities for ET-1, ET-3, S6C, IRL 1620, and BQ123 indistinguishable from the corresponding values for wild-type hET_B (data not shown). The cDNAs encoding Ile-197 → Val hET_B and hET_A were separately subcloned into pGEM7 (Promega); the *Hin*cII/*Eco*RI fragments were isolated from pGEM7/Ile-197 → Val hET_B and pGEM7/hET_A digestions and inserted into *Hin*cII/*Eco*RI-digested pGEM7/Ile-197 → Val hET_B and pGEM7/hET_A encoding the receptor framework from the opposite receptor subtype. The resulting ET receptor chimeras are denoted ABA and BAB, where TMs 4–6 and a portion of TM7 of hET_B or hET_A are inserted into the framework of hET_A and hET_B, respectively. Specifically, chimera ABA is composed of hET_A residues from the amino terminus to Val-180, hET_B residues from Asp-198 to Leu-375, and hET_A residues from Asn-361 to the carboxyl terminus. Chimera BAB is composed of hET_B residues from the amino terminus to Ser-196, hET_A residues from Val-180 to Met-360, and hET_B residues from Asn-376 to the carboxyl terminus. Chimeric constructs were verified by restriction analysis and DNA sequencing, subcloned into pRCCMV, and used to transfect HEK 293 cells as described above.

Cell Harvest and Preparation of Membranes. HEK 293 cells were washed with phosphate-buffered saline (PBS) and released by scraping into PBS/1 mM EDTA. Cells were harvested by centrifugation and rapidly frozen. To prepare crude membranes, frozen cell pellets were thawed on ice, resuspended in 50 mM Hepes, pH 7.5/10 mM $MgCl_2$ (Mg Hepes) containing 0.5 mM phenylmethylsulfonyl fluoride, aprotinin at 5 μg/ml, leupeptin at 5 μg/ml, pepstatin at 5 μg/ml, DNase at 24 μg/ml (Sigma), disrupted by Polytron treatment (two 30-sec bursts at 4°C) with repeated homogenization (4°C), and collected by centrifugation (180,000 × *g* for 40 min at 4°C). The membrane pellet was resuspended in 250 mM sucrose/50 mM Hepes (pH 7.5), washed by a cycle of centrifugation and resuspension, divided into aliquots, and rapidly frozen. Membrane preparations were stable at −70°C for up to 3 mo. Protein was determined by the BCA method (Pierce) using bovine serum albumin as a standard (24).

Radioligand Binding Assays. To determine the apparent K_d for ^{125}I-labeled ET-1, saturation binding assays of HEK 293 cell membranes expressing hET_A or hET_B were conducted and analyzed as described (25). Analysis of the saturation binding data indicated a single class of sites with an apparent K_d of 24 pM and 17 pM for hET_A and hET_B, respectively (data not shown). Competition binding was initiated by addition of membranes (0.33–56.7 μg/ml) from HEK 293 cells transfected with wild-type or hET receptor variants to an assay mixture composed of 0.1% bovine serum albumin/0.12 nM ^{125}I-labeled ET-1 (2200 Ci/mmol; 1 Ci = 37 GBq), and the designated concentration of unlabeled ET-related peptides (American Peptides, Sunnyvale, CA) in Mg Hepes. Binding experiments were conducted for two hr at 37°C; the contents were then filtered and analyzed as described (25). The apparent K_i values are derived from duplicate to quintuplicate experiments using membrane preparations from two independent transfections. Variation in the expression level of the various ET receptors was estimated in preliminary experiments by the specific binding of 0.1 nM ^{125}I-labeled ET-1 and ranged from 33 pmol/mg to 180 fmol/mg. This variation reflects consistent, but different, expression levels for wild-type ET receptors. For certain ET receptor variants, expression levels are reduced relative to wild type; however, reduced expression is not responsible for altered ligand affinities because identical ligand-binding profiles are seen with ET receptor variants that express at wild-type levels or higher. In studies with TM2 mutations of hET_A and hET_B, background binding in HEK 293 membranes contributed a maximum of 13% of specific binding and was due to endogenous ET_A. Due to low expression of chimera ABA, the endogenous receptors in HEK 293 contributed 25% of the specific binding. In this instance, K_i values were determined either by the program LIGAND (26) using a two-binding site analysis or by single-site, nonlinear regression analysis (25) after correcting the specific binding of chimera ABA for the contribution by endogenous ET_A. Both methods resulted in similar K_i values for chimera ABA. The concentration of nonlabeled ET-related peptides was determined by quantitative amino acid analysis; the concentration of ^{125}I-labeled ET-1 was calculated directly by using a constant specific activity (New England Nuclear) due to the catastrophic decay of labeled ligand.

RESULTS

Molecular Modeling. The molecular models built for hET_A and hET_B from the coordinates of BR conserve to a large degree the relative dispositions of the helices in BR. The models therefore display interhelical and cleft regions of substantially the same area as BR. Fig. 1 *Upper* depicts a van der Waals surface on the hET_A model to illustrate the cavities potentially available for ligand binding. Fig. 1 *Lower* is a superposition of the hET_A (cyan) and hET_B (orange) models showing the side chains of residues that differ between the receptor subtypes. The lysine residue conserved between the receptors and implicated in the binding of various peptide agonists (4, 5) and nonpeptide antagonists to hET_B (unpublished work) is located approximately halfway down TM3 and is highlighted in green. Two pairs of residues that differ between hET_A (magenta) and hET_B (yellow) and face the larger of the two clefts, Tyr-129/His-150 within TM2 and Thr-359/Ser-376 within TM7, are indicated. These residues are also located approximately halfway down their respective helices. Due to the functional group differences between histidine and tyrosine, Tyr-129 of hET_A was selected for replacement.

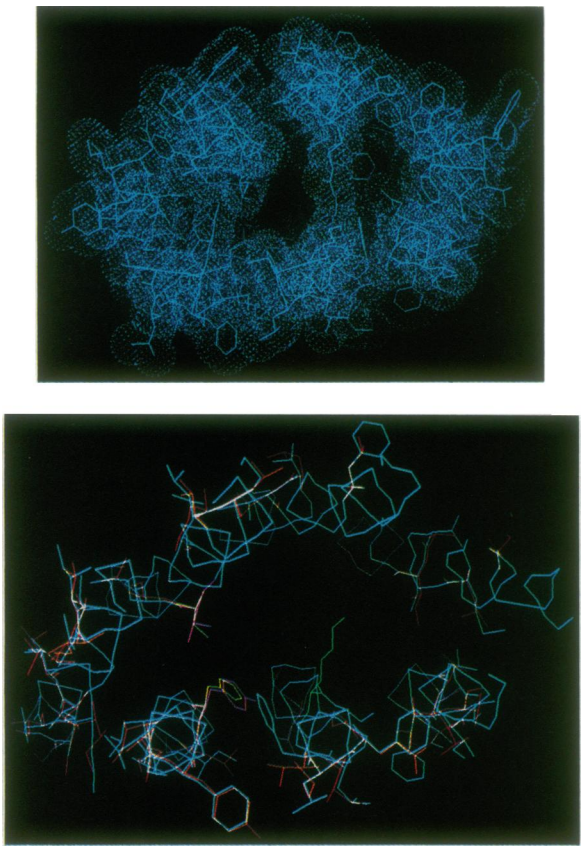

FIG. 1. Models of hET receptors built from coordinates of BR and viewed from the extracellular surface. The view shows TM1 at 9 o'clock with TMs 2–7 following counterclockwise. (*Upper*) Model of hET_A depicted with a van der Waals surface. (*Lower*) Sequence differences between hET_A and hET_B in the TM domains. The hET_A backbone is shown in cyan. Residues differing in hET_B are shown in orange except Lys-166/182 (hET_A/hET_B), which is shown in green, and Tyr-129, Thr-359/His-150, Ser-376 (hET_A/hET_B), shown in magenta and yellow, respectively.

TM2 Mutations. Site-directed mutagenesis was used to replace Tyr-129 of hET_A by alanine, glutamine, asparagine, histidine, lysine, serine, and phenylalanine and to replace His-150 of hET_B by tyrosine and alanine. The resulting receptor variants were evaluated for their apparent binding affinity for peptide antagonist BQ123 and peptide agonists ET-1, ET-2, ET-3, and S6C by competition binding experiments with ^{125}I-labeled ET-1. The ET_B-selective agonist IRL 1620, a linear peptide, was evaluated in four of the mutant receptors.

Fig. 2 highlights a subset of the binding data, depicting the relative abilities of several ligands to compete for ^{125}I-labeled ET-1 binding to Tyr-129 → Phe hET_A, Tyr-129 → His hET_A, His-150 → Tyr hET_B, His-150 → Ala hET_B, and wild-type hET_A and hET_B. The apparent affinities of the ligands for wild-type and mutant receptors are summarized in Table 1. For the wild-type receptors, the affinities of ET-1 and ET-2 are similar; however the ligand selectivity for hET_B over hET_A is pronounced for ET-3, S6C, and IRL 1620. The peptide antagonist BQ123 has the opposite selectivity, substantially favoring hET_A over hET_B. Replacement of Tyr-129 of hET_A generates receptor variants in which the apparent affinity for the hET_B selective agonist peptides ET-3, S6C, and IRL 1620 *increases* substantially (≈140 fold and >10–50 fold in ET-3/S6C and IRL 1620, respectively), whereas the affinities for ET-1 and ET-2 do not change significantly. Concomitantly, the affinity for the ET_A-selective antagonist, BQ123, *decreases* approximately two to three orders of magnitude for the Tyr-129 → Lys, Gln, His, Ala, Asn, or Ser hET_A variants, but only 6-fold for Tyr-129 → Phe hET_A.

In marked contrast, replacement of His-150 of hET_B, the residue in hET_B corresponding to Tyr-129 in hET_A, generates

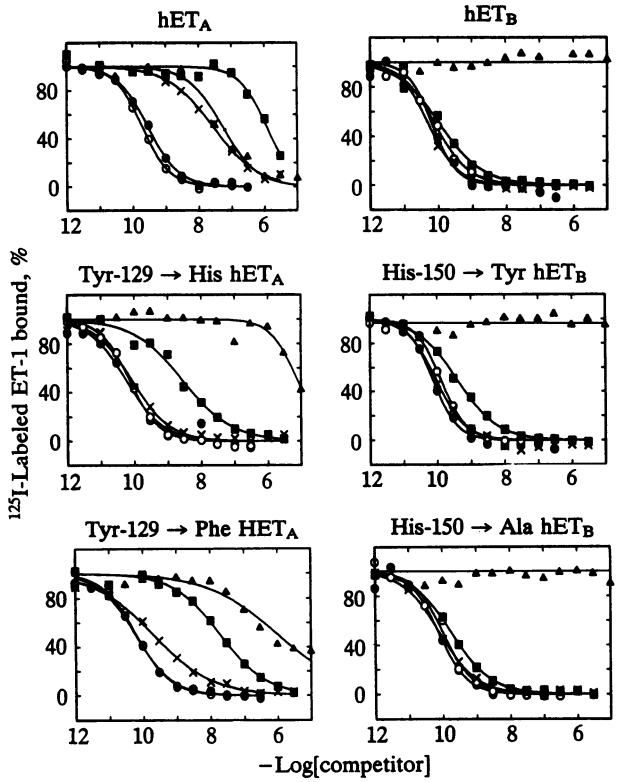

FIG. 2. Competition binding of TM2 variants of ET receptor subtypes. Competitive binding between ^{125}I-labeled ET-1 and unlabeled ET-1 (●), ET-2 (○), ET-3 (×), S6C (■), and BQ123 (▲) to membranes from HEK 293 cells transfected with wild-type hET_A, wild-type hET_B, Tyr-129 → His hET_A, Tyr-129 → Phe hET_A, His-150 → Tyr hET_B, or His-150 → Ala hET_B variants. Data points are the averages of duplicate determinations that usually varied by <7% of total specific binding. A representative data set from the two to five data sets for each ligand/ET receptor variant combination is shown.

Table 1. Binding affinities for TM2 variants of ET receptor

Receptor	Apparent K_i of peptide, nM					
	ET-1	ET-2	ET-3	S6C	BQ123	IRL 1620
WT hET_A	0.018	0.058	6.35	222	13	>1,000*
Y129F hET_A	0.012	0.012	0.031	2.95	76	105
Y129K hET_A	0.016	0.016	0.041	2.59	2,400	ND
Y129A hET_A	0.021	0.034	0.100	1.60	>10,000*	43
Y129N hET_A	0.018	0.021	0.040	1.48	>10,000*	ND
Y129S hET_A	0.017	0.016	0.016	0.68	>10,000*	20
Y129Q hET_A	0.019	0.023	0.037	0.82	1,240	ND
Y129H hET_A	0.017	0.025	0.062	0.56	1,820	ND
WT hET_B	0.012	0.017	0.016	0.029	>10,000*	0.21
H150A hET_B	0.010	0.012	0.009	0.023	>10,000*	0.43
H150Y hET_B	0.013	0.031	0.020	0.075	>10,000*	ND
IYV hET_B	0.009	0.010	0.013	0.031	>10,000*	ND

Competitive binding between ^{125}I-labeled ET-1 and unlabeled ligands was done as described. K_i values were calculated from IC_{50} values determined from nonlinear regression of the competition data (25). K_i values listed are the average of between two and five determinations with membranes prepared from two independent HEK 293 transfections. The maximum range of the K_i values was ±30% of mean values. Lower limits of K_i values are derived from the maximum concentration of ligand used (*). ND, Not determined. WT, wild type. Single-letter amino acid abbreviations are used for receptor designations.

receptor variants (His-150 → Ala and His-150 → Tyr) which have essentially wild-type hET_B affinities for the peptides tested (Fig. 2; Table 1). In hET_B, the residues adjacent to His-150 also differ from those in the corresponding positions in hET_A. To determine whether this triplet of residues contributes to ligand affinity of hET_B, Leu-149, His-150, and Ile-151 of hET_B were simultaneously replaced with the corresponding residues of hET_A (Ile, Tyr, and Val, respectively). The resulting receptor variant, Ile-Tyr-Val hET_B, also has peptide affinities that resemble wild-type hET_B values (Table 1).

Receptor Chimeras. To further evaluate the apparent nonreciprocal effect of receptor substitutions on ligand selectivity, two receptor chimeras between hET_A and hET_B were constructed and evaluated for their ability to bind various agonist and antagonist peptides in I^{125}-labeled ET-1 competition binding assays (Fig. 3). ET receptor chimera ABA is composed of TMs 4–6 and part of TM7 of hET_B within an hET_A framework. The ABA chimera has unaltered affinity for ET-1 but has significantly higher affinities for ET-3, S6C, and IRL 1620 than wild-type hET_A with K_i values for agonist ligands that are similar to wild-type hET_B values (Table 2). In contrast, chimera ABA has an affinity for the ET_A selective antagonist BQ123, which is only 7-fold lower than the value for wild-type hET_A (Table 2).

The reciprocal ET receptor chimera, BAB, where TMs 4–6 and part of TM7 of hET_A are placed within an hET_B framework, has affinities for ET-3, S6C, and IRL 1620 that are decreased one to three orders of magnitude relative to wild-type hET_B but are at least one order of magnitude higher in affinity than wild-type hET_A values (Fig. 3; Table 2). This receptor has no measurable affinity for BQ123.

DISCUSSION

The investigation of receptor features that determine the molecular basis of ligand selectivity represents a fundamental problem in molecular pharmacology and is important for the design of receptor-specific therapeutic agents. In this study, replacement of Tyr-129 within TM2 of hET_A, a residue identified through molecular modeling as potentially important to peptide ligand binding, results in receptor variants that through enhanced binding of several peptide agonists reverse the agonist binding profile from selective to nonselective. These mutants also display a decreased affinity for the cyclic peptide antagonist BQ123, suggesting some degree of overlap of the binding site of this antagonist with that of the agonist peptides with enhanced affinity. In hET_B, replacement of His-150, the residue analogous in sequence to Tyr-129, has no effect on the binding of either agonist peptides or BQ123, indicating that the region of TM2 occupied by Tyr-129/His-150 does not play the same role in the two receptors. Studies with two ET receptor chimeras suggest that residues within TMs 4–6 and part of TM7 of hET_A also contribute significantly to agonist peptide binding. These conclusions are discussed in more detail below.

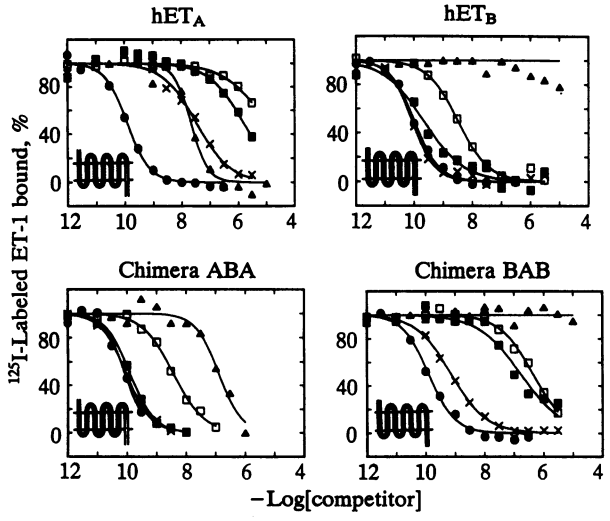

FIG. 3. Competition binding of ET receptor chimeras. Competitive binding between ^{125}I-labeled ET-1 and unlabeled ET-1 (●), ET-3 (×), S6C (■), IRL 1620 (□), and BQ123 (▲) to HEK 293 membranes expressing wild-type hET_A, wild-type hET_B, chimera ABA, or chimera BAB. Data points are the averages of duplicate determinations. For chimera ABA, the total binding of ^{125}I-labeled ET-1 was corrected for the contribution of endogenous ET_A in HEK 293. A representative data set is shown. (*Inset*) TM composition of hET_A (open bar), hET_B (solid bar), and ET receptor chimeras ABA and BAB. The amino termini of the receptors are at left and are extracellular; the carboxyl termini are at right and are intracellular.

Table 2. Binding affinities for chimeric ET receptors

Receptor	Apparent K_i of peptide, nM				
	ET-1	ET-3	S6C	BQ123	IRL 1620
WT hET_A	0.025	5.40	210	4.3	1220
WT hET_B	0.012	0.012	0.018	>1000*	0.33
Chimera ABA	0.017	0.010	0.016	29.9	0.43
Chimera BAB	0.032	0.153	23.0	>1000*	43.2

Competitive binding between ^{125}I-labeled ET-1 and unlabeled ligands was done as described. K_i values were calculated from IC_{50} values determined from nonlinear regression of the competition data (25); K_i values for chimera ABA were calculated as described in text. K_i values listed are the average of two determinations that differed by a maximum of 4-fold between experiments. Lower limits of the K_i values are derived from the maximum concentration of ligand used (*). WT, wild type.

TM2 Mutations of hET_A, Influence of Tyr-129 on Ligand Selectivity. Replacement of a single residue, Tyr-129, within TM2 of hET_A increases binding ≈140-fold for ET-3 and S6C, which modifies the agonist peptide binding affinity to more closely resemble the nonselective profile of hET_B (Fig. 2; Table 1). These results suggest that replacement of Tyr-129 directly or indirectly removes an inhibitory binding interaction, principally by the loss of the phenolic OH group of tyrosine, to increase the affinity of ET-3, S6C, and IRL 1620.

In contrast to the results for the agonist peptides, binding of the cyclic peptide antagonist BQ123 is diminished two to three orders of magnitude for hET_A variants in which Tyr-129 is replaced by alanine, glutamine, asparagine, histidine, lysine, or serine. However, when Tyr-129 is replaced by phenylalanine, the BQ123 affinity decreases only 6-fold (Fig. 2; Table 1). These results are consistent with a key aromatic receptor–ligand interaction for BQ123 binding and suggest that at least a portion of the BQ123 binding site resides within TM2 of hET_A.

Together, these observations indicate that the residue at position 129 of hET_A is a major determinant for agonist peptide selectivity and high affinity binding of the peptide antagonist BQ123. The results suggest that the binding sites for BQ123, ET-3, S6C, and IRL 1620 partially overlap within TM2 of hET_A. This conclusion contrasts sharply with the emerging literature for the cholecystokinin B/gastrin and neurokinin 1 receptors, which suggests that agonist and antagonist binding sites do not overlap appreciably in these peptide GPCRs (27–29).

Two observations suggest that the effect of Tyr-129 replacements on the ligand binding profile of hET_A are specific alterations in receptor/ligand interactions. The apparent affinities for ET-1 and ET-2 are not significantly altered from their wild-type hET_A values; additionally, Tyr-129 → Phe hET_A has a nearly wild-type hET_A affinity for BQ123, in contrast to the two orders of magnitude *increase* in affinity for ET-3 and S6C. These results suggest that the alterations of

ligand affinity and selectivity observed in Tyr-129 hET_A variants are not due to global changes in receptor conformation.

TM2 Mutations of hET_B. Unlike the change in ligand binding profile caused by replacement of Tyr-129 in hET_A, replacement of the corresponding residue in hET_B, His-150, does not affect the binding affinity of agonist or antagonist peptides (Fig. 2; Table 1). The nonreciprocal effect indicates that this region of TM2 within hET_A, but not of hET_B, is important for ligand interaction and suggests that while the affinities of the ET isopeptides may be similar in mutant hET_A and wild-type hET_B, the receptor interactions contributing to binding differ.

Although an aromatic residue is important for high affinity binding of BQ123 to hET_A, conversion of the His-150 region of hET_B to the corresponding hET_A sequence is insufficient to increase the affinity of BQ123 (Fig. 2; Table 1). These results suggest that receptor features in Tyr-150 hET_B and in Ile-Tyr-Val hET_B other than those at or adjacent to Tyr-150 must interfere, either directly or indirectly, with the ability of BQ123 to bind.

Ligand Selectivity of Chimeric ET Receptors. Recently, Sakamoto *et al.* (30) demonstrated that replacement of TMs 4, 5, and 6 of hET_A by the corresponding TMs of hET_B results in a receptor chimera with essentially wild-type hET_B affinities for ET-3 and IRL 1620 and wild-type hET_A affinity for BQ123. Similar findings are obtained with our ABA receptor chimera (Fig. 3; Table 2), which includes, in addition to TMs 4–6, a part of TM7. These results indicate that TMs 1–3 of hET_A are important to BQ123 binding, whereas TMs 4–6 of hET_B are important to ET-3, S6C, and IRL 1620 binding. These observations are consistent with our TM2 mutation data, particularly the insensitivity of agonist ligand affinities to replacement of H150 of hET_B and the importance of Y129 of hET_A for high-affinity binding of BQ123 (Fig. 2; Table 1). However, these data suggest that hET_A regions other than TM2 contribute either directly or indirectly to ligand selectivity.

Our reciprocal ET receptor construct, BAB, has ET-3, S6C, and IRL 1620 affinities that differ significantly from wild-type hET_B values and approach those of hET_A (Fig. 3; Table 2). This indicates that TMs 4-6 and part of TM7 within hET_A contribute to ligand selectivity, but do not fully account for the ligand selectivity of wild-type hET_A. This conclusion is consistent with the TM2 mutations of hET_A where replacement of Y129 alters agonist peptide selectivity to resemble, but not duplicate, the nonselective agonist peptide profile of hET_B (Fig. 2; Table 1). Taken together, these studies indicate that the molecular determinants of hET_A that contribute to ligand selectivity are distributed throughout the receptor sequence; however, the suggested barrel-like structure of the receptor could bring them into spatial proximity.

Implications of Receptor Models. Our hET_A receptor model in conjunction with the results from TM2 mutations suggests that of the two clefts defined by the TM domains (Fig. 1 *Upper*), the larger cleft (bounded by TMs 1, 2, 3, 6, and 7) constitutes a portion of the binding site for agonist ET isopeptides and the antagonist peptide BQ123. The postulated position of Tyr-129 suggests that portions of ET-3, S6C, IRL 1620, and BQ123 penetrate at least halfway into the TM domains and that the interaction surface between these peptide ligands and ET receptors is likely to encompass residues from multiple TM and extracellular domains. Such a large interaction surface could explain the insensitivity of ET-1 and ET-2 to replacement of Tyr-129 of hET_A (Fig. 2; Table 1) if the receptor/ligand interactions within this general binding site differentially contribute to the binding affinity of the various peptide ligands. These data do not exclude, however, the possibility of an alternate binding site (or sites) for ET-1 and ET-2.

The results of this study, while delineating certain interactions responsible for ligand selectivity between ET receptor subtypes, emphasize the molecular complexity of such interactions and suggest that for hET_A, this selectivity may involve multiple receptor regions that act in synergy. This study also highlights the utility of GPCR modeling as a means of identifying receptor residues involved in ligand binding. Although GPCR models based on BR may be approximate, until more definitive structural data are available for membrane-bound receptors, these models in conjunction with receptor mutagenesis studies can provide valuable insight into GPCR/ligand interactions.

We thank Dr. Kenneth Kopple for important discussion and Dr. Ganesh Sathe, Ms. Felicia Watson, and Mr. Rene Morris for synthesis of oligonucleotides and DNA sequencing.

1. Probst, W. C., Snyder, L. A., Schuster, D. I., Brosius, J. & Sealfon, S. C. (1992) *DNA Cell Biol.* **11**, 1–20.
2. Savarese, T. M. & Fraser, C. M. (1992) *Biochem. J.* **283**, 1–19.
3. Baldwin, J. M. (1993) *EMBO J.* **12**, 1693–1703.
4. Mauzy, C., Wu, L. H., Egloff, A. M., Mirzadegan, T. & Chung, F. Z. (1992) *J. Cardiovasc. Pharmacol.* **20**, Suppl. 12, S5–S7.
5. Zhu, G., Wu, L. H., Mauzy, C., Egloff, A. M., Mirzadegan, T. & Chung, F. Z. (1992) *J. Cell. Biochem.* **50**, 159–164.
6. Fathi, Z., Benya, R. V., Shapira, H., Jensen, R. T. & Battey, J. F. (1993) *J. Biol. Chem.* **268**, 14622–14626.
7. Cronet, P., Sander, C. & Vriend, G. (1993) *Protein Eng.* **6**, 59–64.
8. MaloneyHuss, K. & Lybrand, T. P. (1992) *J. Mol. Biol.* **225**, 859–871.
9. Pardo, L., Ballesteros, J. A., Osman, R. & Weinstein, H. (1992) *Proc. Natl. Acad. Sci. USA* **89**, 4009–4012.
10. Trumpp-Kallmeyer, S., Hoflack, J., Bruinvels, A. & Hibert, M. (1992) *J. Med. Chem.* **35**, 3448–3462.
11. Henderson, R., Baldwin, J. M., Ceska, T. A., Zemlin, F., Beckmann, E. & Downing, K. H. (1990) *J. Mol. Biol.* **213**, 899–929.
12. Henderson, R. & Schertler, G. F. X. (1990) *Philos. Trans. R. Soc. London B* **326**, 379–389.
13. Hoflack, J., Trumpp-Kallmeyer, S. & Hibert, M. (1994) *Trends Pharmacol. Sci.* **15**, 7–9.
14. Schertler, G. F. X., Villa, C. & Henderson, R. (1993) *Nature (London)* **362**, 770–772.
15. Sokolovsky, M. (1992) *J. Neurochem.* **59**, 809–821.
16. Elshourbagy, N. A., Korman, D. R., Wu, H. L., Sylvester, D. R., Lee, J. A., Nuthalaganti, P., Bergsma, D. J., Kumar, C. S. & Nambi, P. (1993) *J. Biol. Chem.* **268**, 3873–3879.
17. Takayanagi, R., Ohnaka, K., Takasaki, C., Ohashi, M. & Nawata, H. (1991) *Regul. Pept.* **32**, 23–37.
18. Takai, M., Umemura, I., Yamasaki, K., Watakabe, T., Fujitani, Y., Oda, K., Urade, Y., Inui, T., Yamamura, T. & Okada, T. (1992) *Biochem. Biophys. Res. Commun.* **184**, 953–959.
19. Ihara, M., Noguchi, K., Saeki, T., Fururoda, T., Tsuchida, S., Kimura, S., Fukami, T. R., Ishikawa, K., Nishikibe, M. & Yano, M. (1991) *Life Sci.* **50**, 247–255.
20. Weiner, S. J., Kollman, P. A., Nguyen, D. T. & Case, D. A. (1986) *J. Comput. Chem.* **7**, 230–252.
21. Kunkel, T. A., Roberts, J. D. & Zakour, R. A. (1987) *Methods Enzymol.* **154**, 367–382.
22. Tabor, S. & Richardson, C. C. (1987) *Proc. Natl. Acad. Sci. USA* **84**, 4767–4771.
23. Chen, C. A. & Okayama, H. (1988) *BioTechniques* **6**, 632–638.
24. Smith, P. K., Krohn, R. I., Hermanson, G. T., Mallia, A. K., Gartner, F. H., Provenzano, M. D., Fujimoto, E. K., Goeke, N. M., Olson, B. J. & Klenk, D. C. (1985) *Anal. Biochem.* **150**, 76–85.
25. Elshourbagy, N. A., Lee, J. A., Korman, D. R., Nuthalaganti, P., Sylvester, D. R., Dilella, A. G., Sutiphong, J. A. & Kumar, C. S. (1992) *Mol. Pharmacol.* **41**, 465–473.
26. Munson, P. J. & Rodbard, D. (1980) *Anal. Biochem.* **132**, 220–239.
27. Fong, T. M., Cascieri, M. A., Yu, H., Bansal, A., Swain, C. & Strader, C. D. (1993) *Nature (London)* **362**, 350–353.
28. Gether, U., Johansen, T. E., Snider, R. M., Lowe, J. A., III, Nakanishi, S. & Schwartz, T. W. (1993) *Nature (London)* **362**, 345–348.
29. Beinborn, M., Lee, Y. M., McBride, E. W., Quinn, S. M. & Kopin, A. S. (1993) *Nature (London)* **362**, 348–350.
30. Sakamoto, A., Yanagisawa, M., Sawamura, T., Enoki, T., Ohtani, T., Sakurai, T., Nakao, K., Toyo-oka, T. & Masaki, T. (1993) *J. Biol. Chem.* **268**, 8547–8553.